International Journal of Mass Spectrometry 503 (2024) 117280

Contents lists available at ScienceDirect

International Journal of Mass Spectrometry

journal homepage: www.elsevier.com/locate/ijms

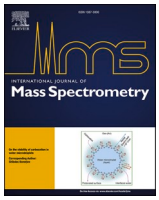

# Laser desorption mass spectrometry of rubrene and photodissociation of its cation

Ian J. Webster, Joshua H. Marks, Michael A. Duncan *

*Department of Chemistry, University of Georgia, Athens, 30602-2556, Georgia*

ARTICLE INFO

*Keywords:*
rubrene
Mass spectrometry
Laser photodissociation
Density functional theory

ABSTRACT

Laser desorption mass spectrometry was employed to study rubrene using three different sample preparation methods. Pressed-pellet and films drop-cast from solution were investigated with a laser-desorption time-of-flight spectrometer. Jet-cooled rubrene cations were produced in a supersonic molecular beam by laser desorption from a film-coated metal rod and detected with time-of-flight mass spectrometry. The films for this process were produced by vacuum sublimation of powder samples. The mass spectra from each of these samples contained the parent molecular ion and fragments resulting from phenyl ring elimination - a pattern similar to that produced by electron impact ionization. The amount of fragmentation varied with sample preparation and desorption laser wavelength. The rubrene cation was mass selected and studied with UV laser photodissociation at 355 nm. The resulting fragmentation mass spectrum indicated the loss of one or two phenyl groups, but no more than this. Computational studies of the ion energetics were used to investigate the stable fragment ion structures and understand the energetics of the dissociation process.

## 1. Introduction

Polycyclic aromatic hydrocarbons (PAHs) are produced by combustion processes in many forms. They are present in environments ranging from candle flames, to automobile exhausts, to interstellar gas clouds [1–8]. Their photochemistry and excited state dynamics have become a recent focus, since these species have found applications in solar cells [9]. Specifically, singlet fission processes exhibited by certain PAH materials provide enhanced solar energy collection and conversion, and rubrene has been investigated extensively in this context [10–15]. The spectroscopy and photochemistry of neutral PAH species are well studied [1,2], but less information is available for the corresponding ions. In the present study, we investigate the energetics and fragmentation behavior of ions produced from rubrene laser desorption mass spectrometry.

Rubrene is one of the most promising organic semiconductors for electronic applications because of its high conductivity and charge mobility. However, rubrene forms crystals with negligible HOMO−LUMO spatial overlap, which inhibits it ability somewhat to undergo singlet fission. Nevertheless, vibronic interactions involving several symmetry-breaking low-frequency vibrational modes enable the energy transfer processes required for this, and rubrene undergoes singlet fission effectively. Thin-film samples have been shown to enhance singlet fission in rubrene, and therefore there is considerable interest in the production, crystallization, and photophysics of such films [16–24]. Laser desorption processes have been employed to produce rubrene films [23,24], but these measurements are lacking diagnostics about the possible photochemistry in the desorption process. In the present study, mass spectrometry investigates the ionized species desorbed from films and their fragmentation products resulting from the laser desorption process using different sample preparation methods and desorption laser wavelengths. Additional measurements investigate the photochemistry of the mass-selected rubrene cation after its desorption.

## 2. Methodology

Rubrene powder, ≥97 % purity, purchased from Sigma-Aldrich was investigated by three different mass spectrometry configurations. In the first, rubrene powder was pressed at high pressure into a pellet and mounted in the source region of a laser desorption time-of-flight mass spectrometer (LD-TOF) [25]. Laser desorption was accomplished with a pulsed Nd:YAG laser operating at either 532 or 355 nm with pulse energies of about 1 mJ in a 1 mm dia. spot. In a thin-film configuration, rubrene powder was dissolved/suspended in methanol and drop-cast

* Corresponding author.
*E-mail address:* maduncan@uga.edu (M.A. Duncan).

https://doi.org/10.1016/j.ijms.2024.117280
Received 23 April 2024; Received in revised form 15 June 2024; Accepted 18 June 2024
Available online 19 June 2024

onto a probe tip which was inserted into the ion source of the same LD-TOF instrument. Again, mass spectra were collected using 532 or 355 nm desorption. In a third configuration, it was necessary to have a film of rubrene on the outside surface of a rotating metal rod for convenient mounting in our molecular beam machine. To achieve this, rubrene powder was loaded into a tungsten boat inside a separate vacuum evaporation/sublimation unit. Resistive heating at ~100 °C under rough vacuum conditions (a few millitorr) produced a sublimed spray of vapor, which was deposited for a period of 12 h on a rotating tungsten rod. The deposition process resulted in an optically thick layer of reddish-colored rubrene coating the tungsten rod. The coated rod was then removed from the vacuum sublimation unit and transferred to a molecular beam machine, where it was mounted in a pulsed-nozzle laser desorption source. Laser desorption was employed at 355 nm with a helium expansion over the desorption position to produce molecular beams of desorbed material, including collisional cooling of the ions produced. This configuration resembles a laser vaporization cluster source [26]. The ions produced by desorption were entrained in the expansion gas and transported through a skimmer into a differentially pumped chamber containing a reflectron time-of-flight mass spectrometer. Pulsed acceleration plates extracted the ions from the molecular beam into the flight tube situated perpendicular to the molecular beam flight direction. This laser desorption/molecular beam configuration has been employed previously for many studies of PAH materials [27–32]. In each of these three desorption configurations, low laser pulse energies (about 1–5 mJ/pulse) were employed to minimize fragmentation. For photodissociation experiments, the rubrene cation was selected with pulsed deflection plates in the flight tube, and excited in the turning region of the reflectron field [33,34]. Its photofragments were analyzed by their flight time through a second flight tube section. In this mode of operation, each ion packet is excited with one laser pulse lasting about 5 nsec as it takes about 1–2 μsec to pass through the reflectron region, and the energy from this one pulse can be absorbed by the cold ions to cause photodissociation. This process is repeated at the 10 Hz repetition rate of the experiment.

Computational studies employed density functional theory (DFT) as implemented in the Gaussian16 program package [35], using the B3LYP functional. All calculations were performed with the def2-TZV basis set with the keyword Opt = tight. The energies presented in this work were zero-point corrected using harmonic frequencies and all structures were confirmed to be true minima.

## 3. Results and discussion

### 3.1. Mass spectra

Fig. 1 shows the mass spectrum produced by Nd:YAG laser desorption of the pressed pellet sample at 532 nm. The spectrum is dominated by a single peak at $m/z = 532$, which is the main isotopic component of the parent molecular ion of rubrene. A small additional mass peak occurs at $m/z$ 455, which corresponds to the loss of a single phenyl ring from the rubrene parent ion. A very similar mass spectrum is obtained for the rubrene thin film produced from solution and desorbed at the same 532 nm laser wavelength. Efficient desorption at the 532 nm wavelength makes sense because of the known absorption spectrum of rubrene, which has a multiplet of broad resonances in the 500 nm region [1]. Absorption in this region gives rubrene its reddish color.

Rubrene has an additional absorption in its spectrum beginning at about 350 nm and extending continuously to higher energy. We investigate excitation in this wavelength region using the 355 nm Nd:YAG laser wavelength. Again, the mass spectra obtained were virtually the same for the pellet and thin film samples, but they differed considerably from the spectra obtained at 532 nm. Fig. 2 shows an example of this for the spectrum of the thin film sample desorbed at 355 nm. The rubrene parent ion at mass 532 is again prominent, as are fragment ions at $m/z =$ 378 and 455. These fragments are easily assigned to the elimination of

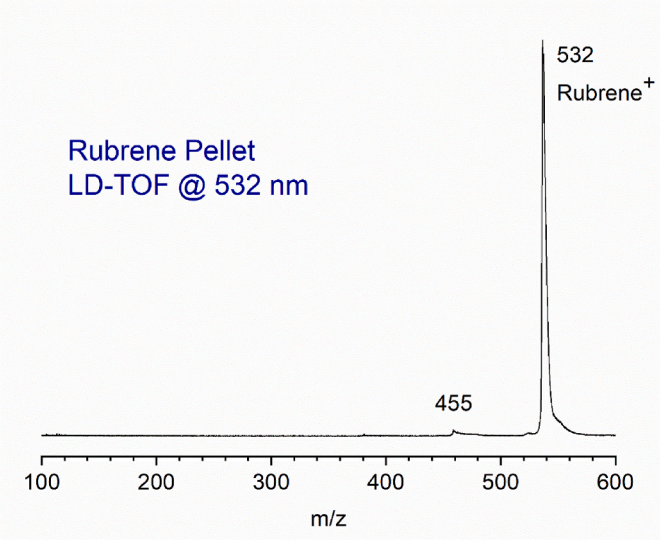


**Fig. 1.** Mass spectrum resulting from laser desorption of a rubrene pressed-pellet sample at 532 nm.

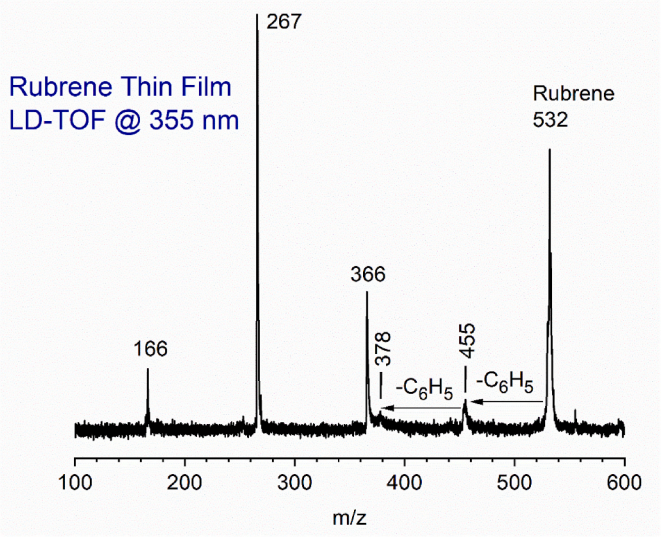


**Fig. 2.** Mass spectrum resulting from laser desorption of a rubrene thin-film sample from drop-casting a solution in methanol at 532 nm.

phenyl groups from the rubrene parent ion. Additional more intense mass peaks are detected at $m/z$ = 166, 267 and 366. Rubrene is synthesized from a triphenyl propargyl alcohol precursor [36]. Removal of the alcohol results in a triphenyl propargyl radical which has a mass of $m/z = 267$, which fragments to form a diphenyl methane cation at $m/z$ = 166. Thionyl chloride is employed in the subsequent dimerization reaction and its complex with the triphenyl propargyl produces $m/z =$ 366. These impurities from the synthesis of rubrene therefore explain the three extra peaks detected. It is interesting that these impurities are only detected at the 355 nm desorption wavelength. Apparently, they do not absorb the 532 nm radiation strongly and are not desorbed and/or ionized at this wavelength. Therefore, the 532 nm desorption laser produces a mass spectrum that is significantly misleading in the purity of the rubrene sample.

Fig. 3 shows the mass spectrum generated from a sublimed film of rubrene when it is desorbed in the laser ablation/molecular beam source at 355 nm and detected with the downstream orthogonal-sampling mass spectrometer. The ions produced are mostly the same as those produced

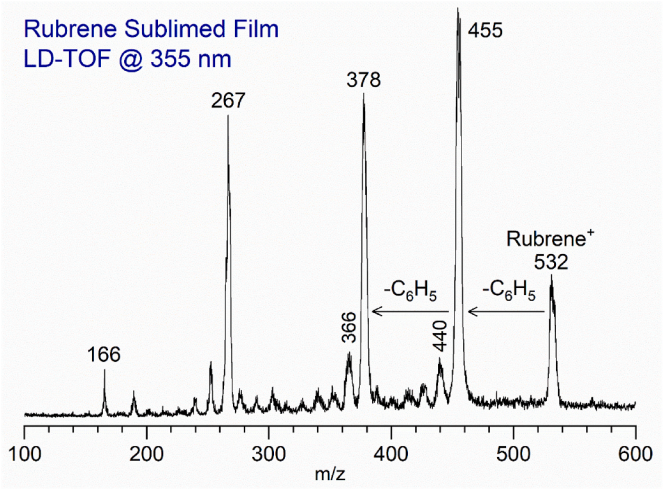


**Fig. 3.** The mass spectrum of rubrene ions produced by laser desorption of a rubrene film coated on a tungsten rod in a supersonic expansion of helium.

by 355 nm desorption from the two other samples, but the intensities of the peaks are different. In particular, the fragment ions at $m/z = 378$ and 455 nm are much more intense relative to the parent ion. However, it is conceivable that this effect is caused by the difference in ion sampling and focusing in the LD-TOF instrument versus the molecular beam instrument. In the LD-TOF experiments the desorbed ions go straight into the flight tube, but in the molecular beam experiment the ions must turn at right angles from the beam into the flight tube. Their velocity in the molecular beam is the same as the helium carrier gas, and this gives them a mass-dependent, off-axis energy that must be compensated for with a deflection plate. This can introduce a focusing bias into the intensities. Another possibility is that the photochemistry is different for the thick-film sublimed sample used in the molecular beam experiment than it is for the thin-film or pellet samples used in the non-beam experiments.

To explore these issues further, it is instructive to consider the mechanisms for ionization and fragmentation in these experiments. The ionization potential of rubrene is 6.41 eV [37]. Its mass spectrum has been studied previously with electron impact ionization [37]. In that data, the parent ion ($m/z = 532$) is prominent and the fragments at $m/z$ 455 and 378 are about 20 and 40 % respectively of the intensity of the parent. These are the same fragment ions seen in laser desorption. The $m/z$ 455 ion is seen in all of the laser desorption measurements, but the $m/z$ 378 fragment is seen most prominently in the data with desorption at 355 nm.

There have been many studies focusing on the mechanism of laser desorption mass spectrometry, but most of them have focused on the mechanism of the MALDI process [38]. Far fewer have focused on the mechanism of neat desorption of films with no matrix. Our research group has investigated the laser desorption process of fullerene films with tunable lasers in the visible, ultraviolet and infrared regions [39]. Enhancements in the desorbed ion yield were found when the desorption laser was tuned into vibrational or electronic resonances. In particular, infrared wavelengths, which have photon energies far too low for photoionization, were found to produce efficient laser desorption and ionization. The ionization was interpreted to arise from electrons desorbed from film impurities that became accelerated by the field in the source region, causing electron-impact ionization in the desorption plume. In that work, careful studies were done with different fields in the source region, and negative-mode mass spectra detected the photodesorbed electrons. A similar mechanism was suggested to take place at visible and UV wavelengths. If this is the case here for these rubrene studies, the similarity in fragmentation patterns for the different wavelengths with those in electron impact ionization is understandable.

We have also recently studied the fragmentation and photo-induced polymerization of various polycyclic aromatic species (pyrene, perylene, coronene) in thin films versus thick pressed pellets [40]. We found that thin-film samples produced minimal fragmentation, whereas thick pellet samples and higher laser powers produced extensive fragmentation and eventual polymerization of PAH species. Those conditions seem to be like the thick films deposited on the rod sample in the molecular beam experiments, which also seemed to produce more fragmentation. However, we detected only trace amounts of any dimerization products in the mass spectra measured here.

It is clear from these experiments on films and pellets that there are several variables affecting mass spectra and fragmentation patterns. The nature of the films not only affects the strength of light absorption, but it also affects the energetics of heating caused by laser absorption. Fragmentation may be caused by light absorption, by film heating or shock waves, and also by electron-impact ionization processes. We therefore further explore this system by eliminating the film environment and studying the photofragmentation of isolated rubrene ions in the gas phase.

### 3.2. Cation photodissociation in the gas phase

To investigate the fragmentation of rubrene ions without the presence of the thin film environment, we use the parent ions ($m/z = 532$) produced by 355 nm laser desorption from the molecular beam source. These ions are collisionally cooled by the supersonic expansion and on the basis of previous work under similar conditions are believed to have temperatures of 20−50K. These ions are laser excited in the turning region of the reflectron time-of-flight mass spectrometer, and the fragment ion masses are determined by the flight time through a second drift tube section of the instrument. This configuration has been employed for many studies of ion fragmentation in our lab [27,28,30,33,34]. Fig. 4 shows the photodissociation of the rubrene cations at 355 nm. The data are recorded in a difference mode of operation in which the signal with the fragmentation laser "off" is subtracted from that with this laser "on." The negative-going signal at $m/z$ 532 therefore shows the destruction of the rubrene cation by laser excitation and the positive signal at $m/z = 378$ and 455 shows the photofragments produced by this laser excitation. It should be noted that the mass resolution in this photofragmentation configuration is worse than that in a normal reflectron time-of-flight instrument. This causes the relatively broad fragment ion mass peaks. Under all conditions, no fragments smaller than $m/z = 378$ are detected.

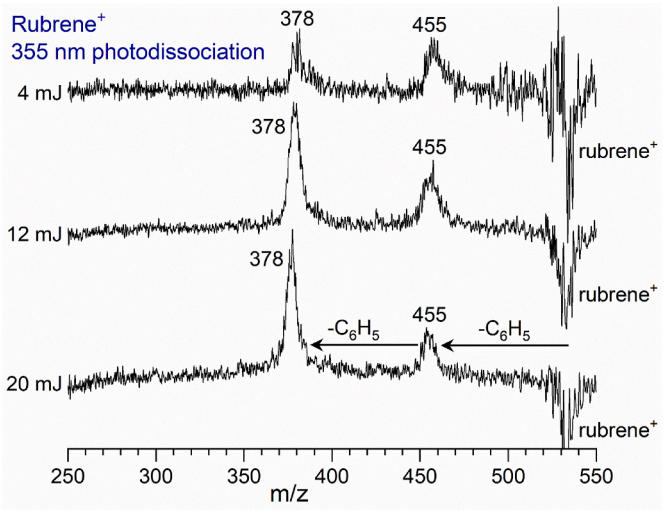


**Fig. 4.** Ultraviolet photodissociation mass spectrum of rubrene cation at varying dissociation laser powers.

To investigate this photochemistry further, we conducted a rudimentary laser power dependence of the signal. A proper power dependence was not possible because of the severe shot-to-shot fluctuations in the signals caused by the desorption process and the gradual removal of material from the sample by the desorption laser. However, we were able to do photodissociation at three different laser pulse energies. Experience with similar systems in the past suggests that multiphoton processes cause a significant variation in the *relative* intensities of different fragment ions at different laser pulse energies, whereas constant relative intensities are consistent with a single photon process. As shown, the laser power dependence here indicates slightly more fragmentation at higher laser pulse energy (i.e., a greater intensity for the $m/z = 378$ peak relative to the $m/z = 455$), but the same two fragment ions are detected in roughly the same intensities from the highest down to the lowest laser power employed. This suggests, but does not prove definitively, that the fragmentation is single-photon. This fragmentation contrasts with that observed previously for many other PAH ions, which dissociate by eliminating hydrogen atoms and usually require multiphoton conditions [41–46].

### 3.3. Computational studies

To further investigate the photodissociation processes of rubrene, we have performed computational studies of the rubrene cation and its possible dissociation fragments. The results of these computations are presented in Table I–V. The rubrene cation energetics are presented in Table I, where it can be seen that the ground state is a doublet, as expected. In these discussions, we use the 0K energetics. The ions are jet-cooled and therefore expected to have cooler internal temperatures. Although "complete" cooling cannot be guaranteed, there is no information to justify any elevated internal temperatures.

The energetic difference between the rubrene neutral and its cation gives a computed ionization potential of 6.1 eV, which compares well with the experimental value of 6.41 eV [37]. The simplest fragmentation process is the elimination of one phenyl group, which produces the triphenyltetracenyl cation at $m/z = 455$. As shown in Table II, the bond dissociation energy required for this process is computed to be 54.3 kcal/mol. A single photon of ultraviolet light at 355 nm has an energy of 80.5 kcal/mol, and therefore this photodissociation process is energetically possible with single photon excitation. There is only one isomer possible for this fragment channel.

The fragment channel detected at $m/z = 378$ corresponds to the loss of two phenyl groups. As shown in Fig. 5, there are three different isomers denoted a, b, c for the resulting diphenyltetracenyl cations corresponding to different positions for the two remaining phenyl groups. Nothing in the experiment allows us to distinguish the structure of the isomer actually produced, but we can discuss their energetics. Tables II and III present the computed energetics for these isomers. From this, it can be seen that isomer a is the most stable and that the energy required to produce this fragment from the triphenyltetracenyl cation is

**Table 1**
ZPVE-corrected relative energies for rubrene ($C_{42}H_{28}$) neutral and cation spin states, as well as those for the neutral fragment species detected. Bond dissociation energies (BDE) are indicated for the elimination of either a phenyl radical (C6H5·) or a biphenyl molecule ($C_{12}H_{10}$) from the rubrene neutral or its cation. Elimination of biphenyl from the cation makes it possible to produce different isomers (a,b,c) of the diphenyltetracenyl cation ($C_{36}H_{23}^+$), as indicated in Fig. 5. Absolute energies are in hartrees and relative energies and bond dissociation energies (BDE) are in kcal/mol. Calculations were performed at the B3LYP/def2-TZV level.

| | 2S + 1 | ZPVE (hartree) | ΔE (kcal/mol) | BDE - phenyl | BDE - biphenyl |
|---|---|---|---|---|---|
| Phenyl | 2 | −231.4854 | 0.00 | – | – |
| | 4 | −231.3174 | +105.4 | – | – |
| | 6 | −231.2049 | +176.0 | – | – |
| Biphenyl | 2 | −463.1431 | 0.00 | – | – |
| | 4 | −463.0357 | +67.4 | – | – |
| | 6 | −462.9127 | +99.2 | – | – |
| Rubrene | 1 | −1616.8056 | 0.00 | 86.5 | 54.9 (a)<br>82.5 (b)<br>110.7 (c) |
| | 3 | −1616.7673 | +24.0 | | |
| | 5 | −1616.6474 | +99.2 | | |
| Rubrene$^+$ | 2 | −1616.5813 | 0.00 | 54.3 | 77.7 (a)<br>78.4 (b)<br>89.4 (c) |
| | 4 | −1616.5050 | +47.83 | 87.9 | |
| | 6 | −1616.3797 | +126.48 | 134.3 | |

**Table 2**
ZPVE-corrected energies for triphenyltetracenyl cation ($C_{36}H_{23}^+$) in different spin states. Absolute energies are in hartrees and relative energies are in kcal/mol. Calculations were performed at the B3LYP/def2-TZV level. Bond dissociation energies (BDE) are those producing either the diphenyltetracenyl cation ($C_{30}H_{18}^+$) in one of it's a, b, c isomeric structures (see Fig. 5) by the loss of phenyl radical or the phenyltetracenyl cation ($C_{24}H_{13}^+$) by the loss of biphenyl from the most stable triphenyltetracenyl cation structure.

| 2S + 1 | ZPVE (hartree) | ΔE (kcal/mol) | BDE - phenyl | BDE - biphenyl |
|---|---|---|---|---|
| 1 | −1385.0093 | 0.00 | 131.5 (a)<br>132.2 (b)<br>143.2 (c) | 128.9 |
| 3 | −1384.9559 | +33.51 | | |
| 5 | −1384.8819 | +79.93 | | |

**Table 3**
ZPVE-corrected and relative energies between diphenyltetracenyl cation ($C_{30}H_{18}^+$) spin states in kcal/mol. Calculations were performed at the B3LYP/def2-TZV level. Bond dissociation energies (BDE) are those producing the phenyltetracenyl cation ($C_{24}H_{13}^+$) from one of the a,b,c isomeric structures (see Fig. 5) by the loss of phenyl radical or the tetracenyl cation ($C_{18}H_8^+$) by the loss of biphenyl from one of the a,b,c isomeric structures.

| 2S + 1 | Geometry | ZPVE (hartree) | ΔE (kcal/mol) | BDE - phenyl | BDE - biphenyl |
|---|---|---|---|---|---|
| 2 | a | −1153.2913 | +14.47 | | |
| 4 | a | −1153.3144 | 0.00 | 105.5 | 61.6 |
| 6 | a | −1153.2391 | +47.25 | | |
| 2 | b | −1153.2951 | +12.09 | | |
| 4 | b | −1153.3132 | +0.69 | 104.8 | 61.1 |
| 6 | b | −1153.2372 | +48.44 | | |
| 2 | c | −1153.2889 | +15.97 | | |
| 4 | c | −1153.2957 | +11.71 | 93.8 | 50.1 |
| 6 | c | −1153.2198 | +59.30 | | |

**Table 4**
ZPVE-corrected and relative energies between phenyltetracenyl cation ($C_{24}H_{13}^+$) spin states in kcal/mol. Calculations were performed at the B3LYP/def2-TZV level. Bond dissociation energies are for the loss of phenyl radical.

| 2S + 1 | ZPVE (hartree) | ΔE (kcal/mol) | BDE |
|---|---|---|---|
| 1 | −921.6557 | +3.25 | 61.2 |
| 3 | −921.6609 | 0.00 | 64.5 |
| 5 | −921.6525 | +5.21 | 59.3 |

**Table 5**
ZPVE-corrected and relative energies between tetracenyl cation ($C_{18}H_8^+$) spin states in kcal/mol. Calculations were performed at the B3LYP/def2-TZV level.

| 2S + 1 | ZPVE (hartree) | ΔE (kcal/mol) |
|---|---|---|
| 2 | −690.0553 | +10.93 |
| 4 | −690.0727 | 0.00 |
| 6 | −689.9878 | +53.29 |

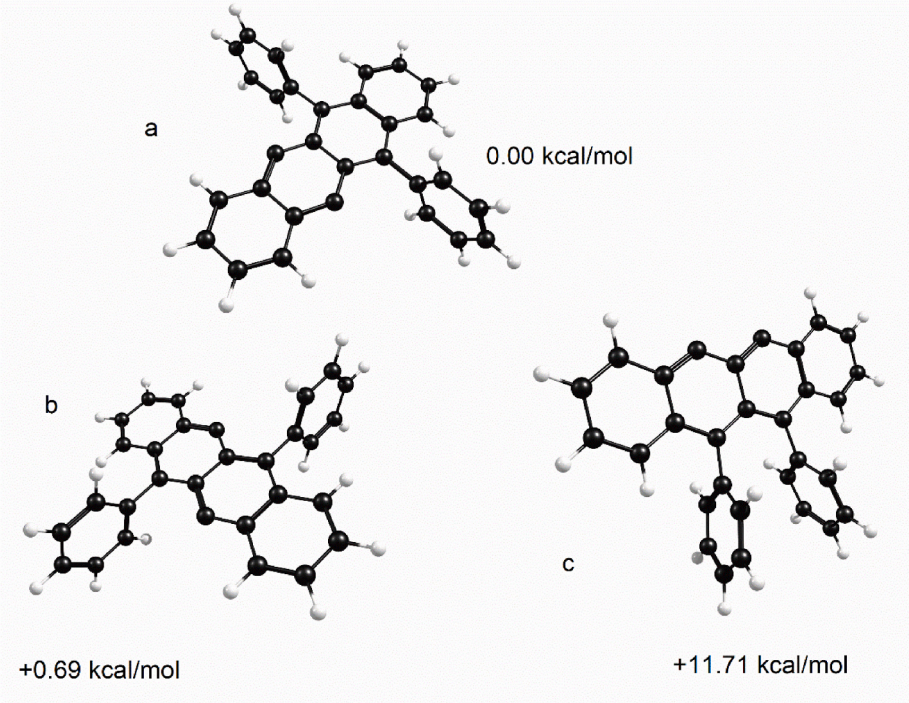


**Fig. 5.** Energetics of fragment ions resulting from rubrene decomposition resulting in the elimination of two phenyl groups producing diphenyltetracenyl isomers.

computed to be 131.5 kcal/mol. The energy for isomer b is almost the same as that for isomer a, whereas that for isomer c is about 12 kcal/mol higher. The minimum amount of energy required to remove first one and then another phenyl group is therefore 54.3 + 131.5 = 185.8 kcal/mol. If the phenyl groups are eliminated sequentially then, the energy required is greater than that of one photon at 355 nm and also greater than that of two of these photons. It could be argued that the ions produced by laser desorption are not cooled efficiently by the supersonic expansion, and that they contain internal energy that could contribute to these photodissociation processes. However, no reasonable assumption for internal energy could make this process possible for one-photon, and two-photon excitation would still require more than an additional 1 eV of internal energy. It is therefore not clear how this fragmentation process can occur efficiently down to very low laser powers.

A solution to this dilemma is that it is possible for the two phenyl groups to be eliminated in a concerted process as a biphenyl molecule. As shown in Table I, the lowest energy path for the loss of biphenyl from rubrene cation, which produces isomer a as the product ion, requires

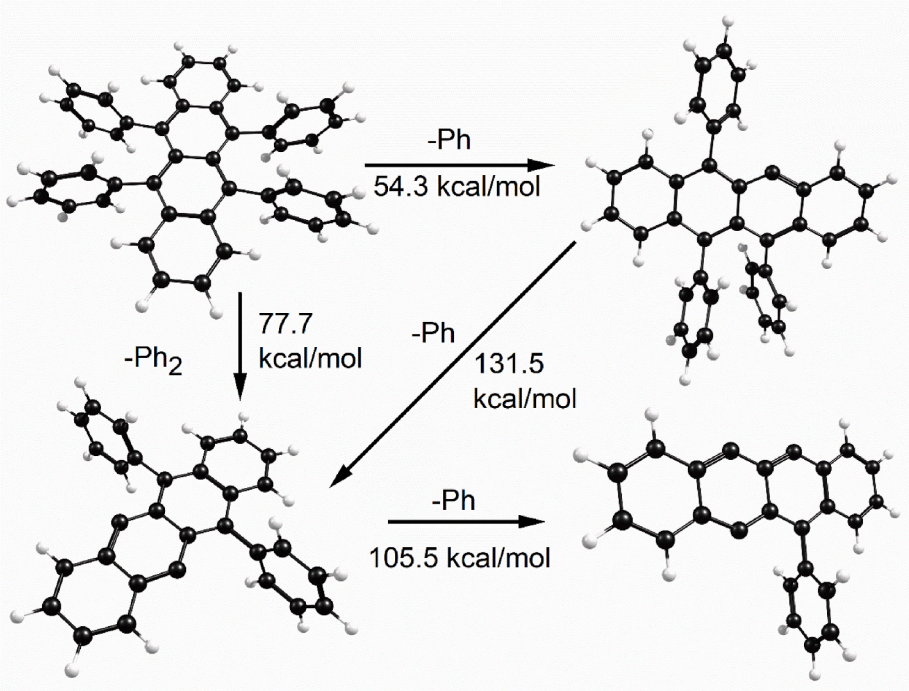


**Fig. 6.** Photodissociation pathways and energy barriers for rubrene cation fragmentation.

only 77.7 kcal/mol, which is possible with a single UV photon at 355 nm. Because no other reasonable scenario is possible, we must conclude that the fragmentation process that produces the $m/z = 378$ fragment ion involves the concerted elimination of a two phenyl radicals in the form of a biphenyl molecule. Fig. 6 summarizes the energetics of these different dissociation pathways for the rubrene system. Because the stability of isomer b is nearly the same as that of isomer a, either or both of these could be produced with single-photon excitation and the elimination of biphenyl. Although it may seem kinetically likely that the two phenyl groups would be eliminated from the same side of the parent ion producing isomer c, this is a higher energy process (higher by 11.7 kcal/mol) and is not energetically possible with one 355 nm photon unless there is significant internal energy in the parent ion. We cannot completely rule out this possibility, and therefore conclude that we do not know which isomer of the diphenyltetracenyl cation is produced. A distribution of isomers a and b seems more likely, but isomer c is also conceivable. The dynamics of how this fragmentation occurs are not possible to investigate with the present instrumentation, but further study of this photochemistry would be quite interesting. Nevertheless, the concerted elimination of biphenyl is required to understand these results.

We also considered the possible dissociation processes that might occur via the absorption of an additional photon. Loss of an additional phenyl group from the diphenyltetracenyl ion to form the phenyltetracenyl ion requires 105.5 kcal/mol, which is more than the energy of an additional 355 nm photon. It is therefore not surprising that we do not see the phenyltetracenyl fragment ion. However, the elimination of a second biphenyl group from the diphenyltetracenyl ion, which would produce a tetracenyl ion without any remaining phenyl groups, requires only 61.6 kcal/mol. This would be possible via the absorption of a second photon. However, we do not see this fragmentation process, even at the highest laser powers. We therefore conclude that the fragmentation processes detected are only those which are possible via the absorption of a single UV photon.

## 4. Conclusion

We have investigated the laser desorption mass spectrometry of rubrene films produced in different ways and desorbed at different wavelengths. We find efficient laser desorption and ionization at both 532 and 355 nm wavelengths that do not vary substantially with the film preparation method. However, the mass spectra vary significantly at the two wavelengths. 532 nm produces only rubrene cations and a small amount of fragmentation, whereas 355 nm produces somewhat more fragmentation and a collection of impurity ions resulting from residual precursor chemicals used in rubrene synthesis. The 532 nm data is therefore misleading with regards to film purity.

Laser photodissociation of rubrene ions desorbed and cooled in a supersonic expansion produces efficient fragmentation at 355 nm. However, the only fragment ions produced are those in which the parent ion has eliminated one or two phenyl groups. Computed energetics indicate that the loss of one phenyl group is possible with a single UV photon. However, the sequential loss of first one and then a second phenyl group is not energetically possible with one photon. Instead, the formation of the abundant fragment ion at $m/z = 378$ is only energetically possible with single photon excitation when the leaving group is a biphenyl molecule. This photochemistry is unanticipated, yet quite efficient.

As shown in Table 1, the computed energetics of fragmentation for neutral rubrene are somewhat comparable to those of its cation. At wavelengths shorter than 520 nm, fragmentation eliminating biphenyl is energetically possible with a single photon. Likewise, at wavelengths shorter than 330 nm, fragmentation via elimination of a single phenyl radical is energetically possible. It seems possible that these processes could affect the photochemistry of rubrene films used for singlet fission. However, light absorption followed by rapid internal energy conversion, which is perhaps likely in solid films, could also conceivably avoid the kind of fragmentation seen here.

## CRediT authorship contribution statement

**Ian J. Webster:** Writing – review & editing, Investigation, Formal analysis. **Joshua H. Marks:** Writing – review & editing, Investigation, Formal analysis, Data curation. **Michael A. Duncan:** Writing – review & editing, Writing – original draft, Supervision, Resources, Project administration, Methodology, Funding acquisition, Formal analysis, Conceptualization.

## Declaration of competing interest

The authors declare that they have no known competing financial interests or personal relationships that could have appeared to influence the work reported in this paper.

## Data availability

Data will be made available on request.

## Acknowledgements

We gratefully acknowledge support of this work by the National Science Foundation through grant no. CHE-2154011.

## References

[1] R.G. Harvey, Polycyclic Aromatic Hydrocarbons, Wiley, New York, 1997.
[2] J. Fetzer, The Chemistry and Analysis of the Large Polycyclic Aromatic Hydrocarbons, John Wiley and Sons, New York, 2007.
[3] T.W. Hartquist, D.A. Williams, *The Molecular Astrophysics of Stars and Galaxies*; International Series on Astron, Clarendon Press, Oxford, 1998.
[4] T. Henning, F. Salama, Carbon in the Universe, Science 282 (1998) 2204.
[5] A.G.G.M. Tielens, The Physics and Chemistry of the Interstellar Medium, Cambridge University Press, Cambridge, 2005.
[6] A.G.G.M. Tielens, Interstellar polycyclic aromatic hydrocarbon molecules, Annu. Rev. Astron. Astrophys. 46 (2008) 289.
[7] B.T. Draine, Physics of the Interstellar and Intergalactic Medium, Princeton University Press, Princeton, 2011.
[8] A.G.G.M. Tielens, The molecular Universe, Rev. Mod. Phys. 85 (2013) 1021.
[9] J. Brédas, J.E. Norton, J. Cornil, V. Coropceanu, Molecular Understandings of organic solar cells: the Challenges, Acc. Chem. Res. 42 (2009) 1691.
[10] M.B. Smith, J. Michl, Singlet fission, Chem. Rev. 110 (2010) 6891.
[11] M.B. Smith, J. Michl, Recent Advances in singlet fission, Annu. Rev. Phys. Chem. 64 (2013) 361.
[12] J.J. Burdett, C.J. Bardeen, The dynamics of singlet fission in crystalline Tetracene and Covalent Analogs, Acc. Chem. Res. 46 (2013) 1312.
[13] D. Casanova, Theoretical Modeling of singlet fission, Chem. Rev. 118 (2018) 7164.
[14] K.M. Felter, F.C. Grozema, Singlet fission in crystalline organic materials: recent Insights and Future Directions, J. Phys. Chem. Lett. 10 (2019) 7208.
[15] L. Ma, K. Zhang, C. Kloc, H. Sun, M.E. Michel-Beyerle, G.G. Gurzadyan, Singlet fission in rubrene single crystal: Direct Observation by Femtosecond Pump-probe spectroscopy, Phys. Chem. Chem. Phys. 14 (2012) 8307.
[16] D. Käfer, L. Ruppel, G. Witte, Ch Wöll, Role of molecular Conformations in rubrene thin film Growth, Phys. Rev. Lett. 95 (2005) 166602.
[17] N. Tuğluoğlu, B. Bariş, H. Gürel, S. Karadeniz, Ö.F. Yüksel, Investigation of optical Band Gap and Device Parameters of rubrene thin film prepared using spin coating Technique, J. Alloy & Compds. 582 (2014) 696.
[18] T.R. Fieltz, R.J. Holmes, Crystal Morphology and Growth in Annealed rubrene thin films, Cryst. Growth Des. 16 (2016) 4720.
[19] M.A. Fusella, F. Schreiber, K. Abbasi, J.J. Ki, A.L. Briseno, B.P. Rand, Homoepitaxy of crystalline rubrene thin films, Nano Lett. 17 (2017) 3040.
[20] R. Jendrzejewski, N. Majewska, S. Majumdar, M. Sawczak, Rubrene thin films with Viably enhanced charge Transport Fabricated by Cryo-Matrix-Assisted laser evaporation, Materials 14 (2021) 4413.
[21] T.S. Volek, Z.T. Armstrong, J.K. Sowa, K.S. Wilson, M.B. Kunz, K. Bera, M. Koble, R. R. Frontiera, P.J. Rossky, M.T. Zanni, Structural Disorder at the Edges of rubrene crystals enhances singlet fission, J. Phys. Chem. Lett. 14 (2023) 11497.
[22] K. Grochowska, S. Majumdar, P. Laukkanen, H.S. Majumdar, M. Sawczak, G. Śliwiński, Pulsed laser deposition of organic semiconductor rubrene thin films, Proc. SPIE 9447 (2015) 94470F.
[23] N. Majewska, M. Gazda, R. Jendrzejewski, S. Majumdar, M. Sawczak, G. Śliwiński, Organic semiconductor rubrene thin films deposited by pulsed laser evaporation of Solidified solutions, Proc. SPIE 10453 (2017) 104532H.

[24] R.J. Thompson, S. Fearn, K.J. Tan, H.G. Cramer, C.L. Kloc, N.J. Curson, O. Mitrofanov, Revealing surface Oxidation on the organic semiconducting single crystal rubrene with time-of-flight secondary ion mass spectrometry, Phys. Chem. Chem. Phys. 15 (2013) 5202.
[25] T.M. Ayers, S.T. Akin, C.J. Dibble, M.A. Duncan, Laser desorption time-of-flight mass spectrometry of Inorganic Nanoclusters: an experiment for Physical Chemistry or Advanced instrumentation Laboratories, J. Chem. Educ. 91 (2014) 291.
[26] M.A. Duncan, Laser vaporization cluster sources, Rev. Sci. Instrum. 83 (2012) 041101.
[27] J.W. Buchanan, J.E. Reddic, G.A. Grieves, M.A. Duncan, Metal and Multi-Complexes with Polyaromatic hydrocarbons: formation and photodissociation of $Fe_x$-$(Coronene)_y$ cations, J. Phys. Chem. A 102 (1998) 6390.
[28] J.W. Buchanan, G.A. Grieves, J.E. Reddic, M.A. Duncan, Novel Mixed-Ligand Sandwich Complexes: Competitive Binding of Iron with Benzene, coronene and $C_{60}$, Int. J. Mass Spectrom. 182 (1999) 323.
[29] M.A. Duncan, A.M. Knight, Y. Negeshi, S. Nagoa, Y. Nakamura, A. Kato, A. Nakajima, K. Kaya, Production of jet-cooled coronene and coronene cluster Anions and their study with Photoelectron spectroscopy, Chem. Phys. Lett. 309 (1999) 49.
[30] N.R. Foster, G.A. Grieves, J.W. Buchanan, N.D. Flynn, M.A. Duncan, Growth and photodissociation $Cr_x(Coronene)_y$ Complexes, J. Phys. Chem. A 104 (2000) 11055.
[31] T.M. Ayers, B.C. Westlake, M.A. Duncan, Laser Plasma production of metal and metal-Compound Complexes with PAH's, J. Phys. Chem. A 108 (2004) 9805.
[32] T.M. Ayers, B.C. Westlake, D.V. Preda, L.T. Scott, M.A. Duncan, Laser Plasma production of metal-Corannulene ion-molecule Complexes, Organometallics 24 (2005) 4573.
[33] K. LaiHing, T.G. Taylor, P.Y. Cheng, K.F. Willey, M. Peschke, M.A. Duncan, Photodissociation in a reflectron time-of-flight mass spectrometer: a Novel MS/MS Scheme for high mass systems, Anal. Chem. 61 (1989) 1458.
[34] D.S. Cornett, M. Peschke, K. LaiHing, P.Y. Cheng, K.F. Willey, M.A. Duncan, A reflectron time-of-flight mass spectrometer for laser photodissociation, Rev. Sci. Instrum. 63 (1992) 2177.
[35] M.J. Frisch, G.W. Trucks, H.B. Schlegel, G.E. Scuseria, M.A. Robb, J.R. Cheeseman, G. Scalmani, V. Barone, G.A. Petersson, H. Nakatsuji, X. Li, M. Caricato, A. V. Marenich, J. Bloino, B.G. Janesko, R. Gomperts, B. Mennucci, H.P. Hratchian, J. V. Ortiz, A.F. Izmaylov, J.L. Sonnenberg, D. Williams-Young, F. Ding, F. Lipparini, F. Egidi, J. Goings, B. Peng, A. Petrone, T. Henderson, D. Ranasinghe, V. G. Zakrzewski, J. Gao, N. Rega, G. Zheng, W. Liang, M. Hada, M. Ehara, K. Toyota, R. Fukuda, J. Hasegawa, M. Ishida, T. Nakajima, Y. Honda, O. Kitao, H. Nakai, T. Vreven, K. Throssell, J.A. Montgomery Jr., J.E. Peralta, F. Ogliaro, M. J. Bearpark, J.J. Heyd, E.N. Brothers, K.N. Kudin, V.N. Staroverov, T.A. Keith, R. Kobayashi, J. Normand, K. Raghavachari, A.P. Rendell, J.C. Burant, S.S. Iyengar, J. Tomasi, M. Cossi, J.M. Millam, M. Klene, C. Adamo, R. Cammi, J.W. Ochterski, R.L. Martin, K. Morokuma, O. Farkas, J.B. Foresman, D.J. Fox, Gaussian 16, Revision C.01, Gaussian, Inc., Wallingford CT, 2016.
[36] B. Furniss, Vogel's Textbook of Practical Organic Chemistry, fifth ed., Longman Scientific & Technical: Essex, England, 1989.
[37] NIST Chemistry WebBook, NIST Standard Reference Database Number 69, Eds. P.J. Linstrom and W.G. Mallard, National Institute of Standards and Technology, Gaithersburg MD, 20899, https://doi.org/10.18434/T4D303, (retrieved March 28, 2024).
[38] R.B. Cole, Electrospray and MALDI Mass Spectrometry, second ed., Wiley, Hoboken, NJ, 2010.
[39] T.C. Cheng, S.T. Akin, C.J. Dibble, S. Ard, M.A. Duncan, Tunable infrared laser desorption and ionization of fullerene films, Int. J. Mass Spectrom. 354–355 (2013) 159.
[40] I.J. Webster, J.L. Beckham, N.D. Johnson, M.A. Duncan, Photochemical synthesis and spectroscopy of Covalent PAH Dimers, J. Phys. Chem. A 126 (2022) 1144.
[41] H.W. Jochims, E. Rühl, H. Baumgärtel, S. Tobita, S. Leach, Size effects on dissociation rates of polycyclic aromatic hydrocarbon cations: Laboratory studies and Astrophysical Implications, Astrophys. J. 420 (1994) 307.
[42] S.P. Ekern, A.G. Marshall, J. Szczepanski, M. Vala, Photodissociation of gas-phase polycyclic aromatic hydrocarbon cations, J. Phys. Chem. A 102 (1998) 3498.
[43] A. Petrignani, M. Vala, J.R. Eyler, A.G.G.M. Tielens, G. Berden, A.F.G. van der Meer, B. Redlich, J. Oomens, Breakdown products of Gaseous polycyclic aromatic hydrocarbons investigated with infrared ion spectroscopy, Astrophys. J. 826 (2016) 33.
[44] B. West, S.R. Castillo, A. Sit, S. Mohamad, B. Lowe, C. Joblin, A. Bodi, P.M. Mayer, Unimolecular reaction energies for polycyclic aromatic hydrocarbon ions, Phys. Chem. Chem. Phys. 70 (2018) 7195.
[45] P. Castellanos, A. Candian, J. Zgen, H. Linnartz, A.G.G.M. Tielens, Photoinduced polycyclic aromatic hydrocarbon Dehydrogenation. The Competition between H- and $H_2$-loss, Astron. Astrophys. 616 (2018) A166.
[46] J. Zhen, T. Chen, A.G.G.M. Tielens, Laboratory photochemistry of pyrene clusters: an efficient way to form Large PAHs, Astrophys. J. 863 (2018) 128.